Chiral (Diphosphonite)platinum Complexes in Asymmetric Hydroformylation

by **Ruben van Duren**[a]), **Leandra L. J. M. Cornelissen**[a]), **Jarl Ivar van der Vlugt**[a]), **Jeroen P. J. Huijbers**[a]), **Allison M. Mills**[b]), **Anthony L. Spek**[b]), **Christian Müller**[a]), and **Dieter Vogt***[a])

[a]) Schuit Institute of Catalysis, Laboratory for Homogeneous Catalysis, Eindhoven University of Technology, Den Dolech 2, NL-5600 MB Eindhoven
(phone: +31 40 247 2483; fax: +31 40 2455054; e-mail: d.vogt@tue.nl)
[b]) Crystal and Structural Chemistry, Utrecht University, Padualaan 8, NL-3584 CH Utrecht

Dedicated to Professor *Giambattista Consiglio* on the occasion of his 65th birthday

The chiral diphosphonite ligand (11b*R*,11′b*R*)-4,4′-(9,9-dimethyl-9*H*-xanthene-4,5-diyl)bis[dinaphtho[2,1-*d*:1′,2′-*f*][1,3,2]dioxaphosphepin] ((*R*,*R*)-XantBino; (*R*)-**1**), based on a rigid xanthene backbone, was applied in the Pt/Sn-catalyzed hydroformylation of styrene (**4a**), 4-methylstyrene (**4b**), vinyl acetate (**4c**), and allyl acetate (**4d**), by using a Pt/Sn ratio of 1:1. High ee of up to 80% were observed, along with good regioselectivities towards the desired branched aldehydes. For styrene, an interesting inversion in the stereoselection process was observed at elevated temperatures, and a mechanism is proposed considering the temperature dependence of the regioselectivity. The complex $[PtCl_2\{(S,S)\text{-XantBino}\}]$ ((*S*)-**2**) was characterized by X-ray crystal-structure analysis, revealing an unusual out-of-plane ligand coordination of the metal fragment. The complex $[PtCl(SnCl_3)\{(R,R)\text{-XantBino}\}]$ ((*R*)-**3**) was characterized by means of ^{31}P-NMR spectroscopy.

Introduction. – The asymmetric hydroformylation of alkenes is a reaction of great potential for the production of optically active aldehydes, which are versatile building blocks in synthetic organic chemistry [1][2]. Initial work on asymmetric hydroformylation in the presence of cobalt [3], platinum [4], and rhodium catalysts [5] resulted in very low enantioselectivities, but the Pt/Sn-catalyst, modified with chiral diphosphine ligands and pioneered by *Consiglio* and co-workers led to much better results than any previous system [6]. However, these catalysts showed poor regioselectivities, yielding the branched, chiral aldehydes in only 50–70% and in some cases of up to 80% [7]. Additionally, the formation of hydrogenated products and double-bond isomerization as unwanted side reactions were observed.

Typically, a large excess of up to 6 equiv. of $SnCl_2$ was necessary to form stable catalysts and to avoid decomposition to Pt-black. However, this excess causes significant product racemization, as observed problem for the early systems, leading to lower overall enantioselectivities [6]. To overcome these drawbacks, trapping agents, *e.g.*, triethyl orthoformate ($HC(OEt)_3$) were added, to achieve *in situ* protection of the aldehyde and to reach high enantioselectivities of up to 96% [8][9]. Alternatively, preformation of the Pt/Sn bimetallic catalyst species resulted in higher enantioselectivities as well as chemo- and regioselectivities [10][11].

In recent years, research on asymmetric hydroformylation has mainly focused on Rh-systems, even though they generally displayed poor enantioselectivities but higher activities and regioselectivities for a long time [12]. Only recently, the phosphino-phosphite ligand (*R*,*S*)-binaphos, introduced by *Takaya* and co-workers [13], and the large-bite-angle diphosphites independently introduced by *Babin* and *Whiteker* [14] and *van Leeuwen* and co-workers [15] led to real breakthroughs.

We recently became interested again in the Pt/Sn catalysts because of their isomerization activity, which can be highly beneficial in the hydroformylation of internal alkenes. In fact, large-bite-angle diphosphine ligands with a rigid xanthene backbone give very stable and selective catalysts for the Pt-catalyzed hydroformylation of alkenes [16]. We already successfully prepared and applied chiral xanthene-based diphosphonite ligands in the nickel-catalyzed asymmetric hydrocyanation [17] and the rhodium-catalyzed asymmetric hydroformylation [18]. Here, we report on the use of the chiral diphosphonite ligand (*R*,*R*)-XantBino ((*R*)-**1**) [19] in the Pt/Sn-catalyzed asymmetric hydroformylation of styrene (**4a**), 4-methylstyrene (**4b**), vinyl acetate (**4c**), and allyl acetate (**4d**). Phosphonite ligands in general have only rarely been applied in homogeneous catalysis [20–27], and the use of diphosphonites in hydroformylation reactions has been very limited so far [28–30]. Recent studies on Pt/Sn-catalyzed asymmetric hydroformylation employed diphosphite ligands [31], but only one report has dealt with the use of chiral diphosphonites in Pt-catalyzed asymmetric hydroformylations, to the best of our knowledge [28].

Results and Discussion. – The chiral diphosphonite ligands (*R*,*R*)-XantBino ((*R*)-**1**) [17][19] and (*S*,*S*)-XantBino ((*S*)-**1**) were treated with $[PtCl_2(MeCN)_2]$ or $[PtCl_2(cod)]$ (cod = cycloocta-1,5-diene), affording the corresponding Pt-complexes $[PtCl_2\{(R,R)$-XantBino$\}]$ ((*R*)-**2**) and $[PtCl_2\{(S,S)$-XantBino$\}]$ ((*S*)-**2**), as white solids (*Fig. 1*) in good yields. The ^{31}P-NMR spectrum of complex (*S*)-**2** showed 2 *d* at δ 110.5 and 113.1 with ^{195}Pt satellites, and coupling constants $J(P,P) = 15.9$ Hz and $J(Pt,P) = 5000$ and 5040 Hz were observed. Apparently, (*S*)-**2** is devoid of the C_2 symmetry shown in *Fig. 1*, suggesting that the inequivalency of the two P-atoms is due to a distorted conformation around the metal center. Furthermore, the observed coupling constants clearly indicate *cis*-coordination of the diphosphonite ligand towards the Pt-center [18][28][32]. Similar ligands of the Xantphos family are known to form monomeric Pt-complexes with both *cis*- and *trans*-coordination [16][33–35].

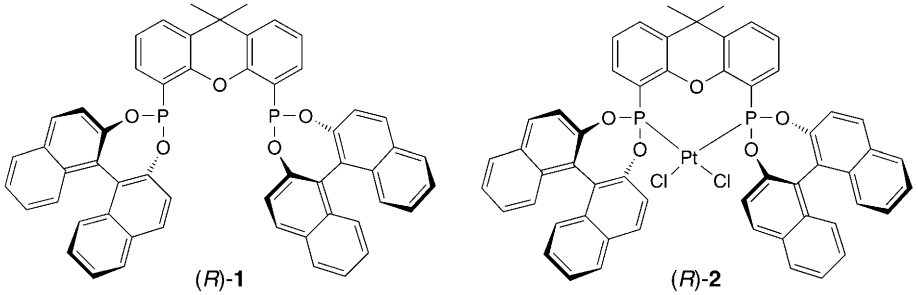

Fig. 1. *(*R,R*)-XantBino* ((*R*)-**1**) *and [PtCl$_2${(*R,R*)-XantBino}]* ((*R*)-**2**)

We were able to obtain single crystals of complex (*S*)-**2**, suitable for X-ray crystal-structure analysis, by layering a CH_2Cl_2 solution of (*S*)-**2** with MeCN. The molecular structure is depicted in *Fig. 2*, with selected bond lengths and angles listed in *Table 1*.

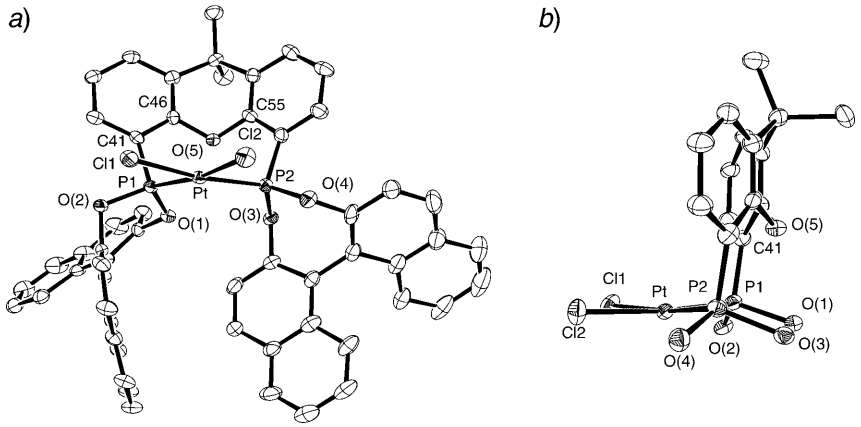

Fig. 2. a) *Molecular Structure of* (*S*)-**2**. b) *Detail of Backbone and Metal Fragment*. Displacement ellipsoids are drawn at the 50% probability level; H-atoms are omitted for clarity[1]).

Table 1. *Selected Bond Lengths, Distances, and Bond Angles for* (S)-**2**

Bond lengths [Å]				Angles [°]			
Pt–P(1)	2.2229(11)	Pt–P(2)	2.2245(11)	Cl(1)–Pt–Cl(2)	87.99(4)	P(1)–Pt–P(2)	99.64(4)
Pt–Cl(1)	2.3504(11)	Pt–Cl(2)	2.3450(11)	Cl(1)–Pt–P(1)	84.32(4)	Cl(1)–Pt–P(2)	172.19(4)
P(1)–O(1)	1.604(3)	P(1)–O(2)	1.601(3)	Cl(2)–Pt–P(2)	87.39(2)	Cl(2)–Pt–P(1)	170.59(4)
P(2)–O(3)	1.603(3)	P(2)–O(4)	1.616(3)	O(1)–Pt–O(2)	102.54(14)	O(3)–Pt–O(4)	102.61(17)
P(1)–P(2)	3.398	Pt–O(5)	3.335(3)	C(46)–O(5)–C(55)	112.6(3)	C(45)–C(47)–C(50)	105.7(4)

The molecular structure of (*S*)-**2** shows a slightly distorted square-planar geometry around the Pt-center, as is evident from the angle P(1)–Pt–P(2) of 99.64(4)° [18b]. The distance between the Pt-atom and the O-atom of the xanthene backbone is 3.335(3) Å, which is too large to assume any bonding interaction. The Pt–P bond lengths of 2.2229(11) (Pt–P(1)) and 2.2245(11) Å (Pt–P(2)), respectively, are similar to those observed in other (phosphonite)platinum complexes [22][28][36–38]. The arrangement around the two P-atoms is depicted in *Fig. 2,a*. While one of the binaphthalene moieties is oriented parallel to the xanthene backbone, the other one is orthogonal to this backbone. This is in agreement with the observed inequivalency of the two P-atoms observed in the ^{31}P-NMR spectrum, establishing the existence of similar conformations in solution and in the solid state. The dihedral angle between the plane Cl(1)–Pt–Cl(2) and the backbone plane P(1)–P(2)–C(41)[1]) is 112.2°. This shows that the Pt-atom is located outside of the plane consisting of the backbone and the P-atoms, as can

[1]) Arbitrary atom numbering; for the systematic name, see the *Exper. Part.*

be seen in *Fig. 2, b* (the binaphthalene units are omitted for clarity). This unusual coordination behavior is in clear contrast to other known examples of xantphos-type metal complexes, where the central atom is in the plane with the backbone (for comparison with Pt–P bond lengths for phosphines, see [37a, b]; for (phosphite)platinum complexes, see [37c]). This 'out-of-plane' Pt-atom gives rise to a high accessibility to the metal center and should, therefore, increase the activity in catalytic reactions.

Reaction of the complex [$PtCl_2$\{(*R*,*R*)-XantBino\}] ((*R*)-**2**) with 1 equiv. of $SnCl_2$ in CH_2Cl_2 led to a yellow solution of the corresponding Pt/Sn complex [$PtCl(SnCl_3)$\{(*R*,*R*)-XantBino\}] ((*R*)-**3**). After concentrating the solution of the complex, it was characterized by its ^{31}P-NMR spectroscopy at $-50°$ (*Fig. 3*). Two *d* with J(P,P) = 15.2 Hz were observed for the two inequivalent P-atoms as main resonances at δ 124.7 and 132.8 (P_o and P_x). The corresponding Pt-satellites are labeled with x and o, respectively. Apparently, insertion of $SnCl_2$ occurs preferentially only in one of the two Pt–Cl bonds, since two isomers are expected due to the lack of C_2 symmetry of the starting material. The presence of only one isomer indicates that insertion of $SnCl_2$ into the Pt–Cl bond either determines the orientation of the two binaphthalene moieties, or that an average signal of the two P-nuclei is observed even at $-50°$. Interestingly, coupling of the P-atoms, which differ substantially due to their *cis*- and *trans*-position relative to the $SnCl_3$ ligand, with the ^{119}Sn and ^{117}Sn nuclei can also be observed. *Table 2* summarizes the oberved coupling constants; the assignment is based on a literature example with P-based ligands [39].

We applied the chiral diphosphonite ligand (*R*)-**1** in the Pt/Sn-catalyzed asymmetric hydroformylation of styrene (= ethenylbenzene; **4a**), 4-methylstyrene (= 1-ethenyl-4-

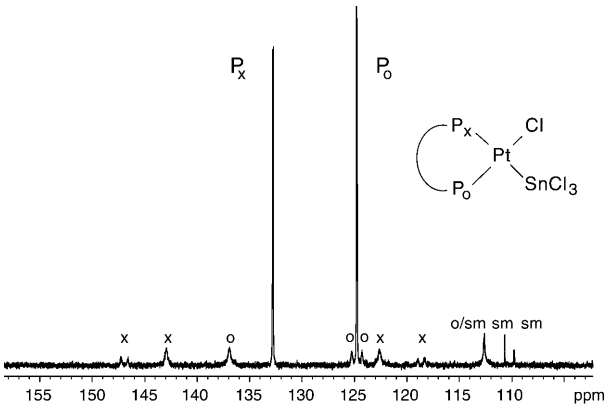

Fig. 3. *^{31}P-NMR Spectrum of [PtCl($SnCl_3$){(*R*,R)-XantBino}]* ((*R*)-**3**) *in CH_2Cl_2 and the Corresponding Assignment.* sm: starting material (*R*)-**2**.

Table 2. *Assignment of Signals in the ^{31}P-NMR Spectrum of (*R*)-**3**.* δ in ppm, J in Hz.

	δ(P)	J(P,Pt)	J(P,Sn)	J(P,P)
P_o	124.7	4909	197	15.2
P_x	132.8	4108	5856, 5596	15.2

methylbenzene; **4b**), vinyl acetate (=ethenyl acetate; **4c**), and allyl acetate (=prop-2-enyl acetate; **4d**). For this, complex (*R*)-**2** was pretreated with $SnCl_2$ in CH_2Cl_2 and the resulting solution containing the precatalyst (*R*)-**3** was used in the catalysis experiments (*Scheme 1*). As already mentioned, an excess of $SnCl_2$ can lead to racemization of the formed aldehyde **5**, which results in a decrease of the enantioselectivity with increasing conversion [9][10]. By using rigid large-bite-angle ligands, however, the amount of side reactions can be reduced considerably, even if only 1 equiv. of $SnCl_2$ with respect to Pt-complex (*R*)-**2** is used [16]. *Table 3* summarizes the results of the hydroformylation of styrene (**4a**) with (*R*)-**3** at 20°, showing indeed no considerable change in the ee with conversion. The same holds for the regioselectivity, which remains high at 80% (ratio **5a**/**6a**). These results show that the (diphosphonite)platinum/$SnCl_2$ complex (*R*)-**3** remains stable during the course of the catalytic reaction and does not lead to any racemization of the product at room temperature.

Scheme 1. *Pt/Sn-Catalyzed Hydroformylation of Prochiral Alkenes*

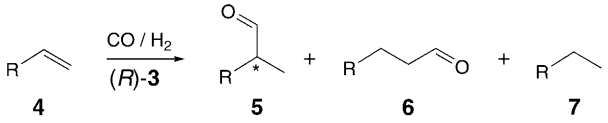

a R = Ph; **b** R= 4-Me–C_6H_4; **c** R = AcO; **d** R = $AcOCH_2$

Table 3. *Enantioselective Hydroformylation of Styrene* (**4a**) *with* (R)-**3** *as a Function of Conversion*[a])

t [h]	Conversion [%]	Hydrogenation [%][b])	b/l[c])	ee (config.) [%]
4	4	46	80:20	26 (*R*)
6	6	39	80:20	26 (*R*)
10	15	27	79:21	27 (*R*)
10[d])	100	18	77:23	27 (*R*)

[a]) Reaction conditions: 20°, 20 bar, ligand/Pt 1:1, $SnCl_2$/Pt 1:1, substrate/Pt 1000:1, CO/H_2 1:1, CH_2Cl_2; preformation 2 h at 20 bar, 60°. [b]) Formation of **7a**. [c]) Ratio **5a**/**6a**, *i.e.*, branched/linear aldehyde. [d]) Substrate/Pt 170:1.

An interesting observation is the fact that the amount of hydrogenation by-product **7a** decreases with increasing conversion, suggesting that a different catalytic species, only present at the beginning of the reaction, is responsible for this side reaction (*Table 3*). During our studies, a short induction period of *ca.* 30 min was indeed recognized, which could explain the observed results. Similar observations were made in earlier studies of the Pt/Sn-catalyst systems [40].

To study the influence of temperature and pressure on the catalyst performance, these parameters were varied from 0 to 100° and from 10 to 60 bar, respectively. The obtained data are summarized in *Table 4*. As expected, the productivity (TON=turnover number) decreases with increasing pressure, as the coordination of styrene to the metal center requires dissociation of carbon monoxide. Compared to reaction rates with Xantphos [34], the increased activity of this type of catalyst agrees well with the

Table 4. *Enantioselective Hydroformylation of Styrene* (**4a**) *with (*R*)-***3***[a])*

p [bar]	*T* [°]	*t* [h]	Conversion [%]	Hydrogenation [%][b])	b/l[c])	ee (config.) [%]	TON
10	20	15	43	47	83:17	18 (*R*)	430
10	40	10	87	42	78:22	9 (*R*)	870
10	60	5	99	52	63:37	3 (*S*)	999
10	80	2	83	64	45:55	6 (*S*)	830
10	100	0.5	58	78	34:66	4 (*S*)	580
20	0	64	23	35	69:31	30 (*R*)	230
20	20	15	45	37	79:21	27 (*R*)	450
20	40	10	99	39	79:21	17 (*R*)	999
20	60	5	90	40	73:27	10 (*R*)	900
20	80	2	95	53	57:43	1 (*S*)	950
20	100	0.5	61	68	45:55	2 (*S*)	610
60	20	10	12	26	71:29	14 (*R*)	120
60	40	4	21	25	73:27	8 (*R*)	210
60	60	1.75	36	25	74:26	3 (*S*)	360
60	80	0.5	35	36	70:30	2 (*S*)	350

[a]) Reaction conditions: ligand/Pt/$SnCl_2$ 1:1:1, substrate/Pt 1000:1, CO/H_2 1:1, CH_2Cl_2; preformation: 2 h at 20 bar, 60°. [b]) Formation of **7a**. [c]) Ratio **5a**/**6a**, *i.e.*, branched/linear aldehyde.

higher accessibility of the metal due to the 'out-of-plane' Pt-center. The lower linear-to-branched ratio supports this even further.

Interestingly, at higher pressure, *i.e.*, higher H_2 partial pressure, the hydrogenation reaction towards ethylbenzene (**7a**) is reduced (*Table 4*). This suggests that the transition state for hydroformylation contains at least one more CO compared to the transition state for hydrogenation (*Scheme 2*). Therefore, the reaction path is influenced by the partial pressure of CO [41]. As hydrogenation increases at higher reaction temperatures, this process is predominantly governed by a larger temperature dependence of the first-order reaction (alkyl formation and β-hydride elimination) compared to the competing second-order reaction (acyl formation and acyl hydrogenolysis towards the hydroformylation product) [41].

Scheme 2. *Hydroformylation* vs. *Hydrogenation*. Only the formation of the linear product is shown.

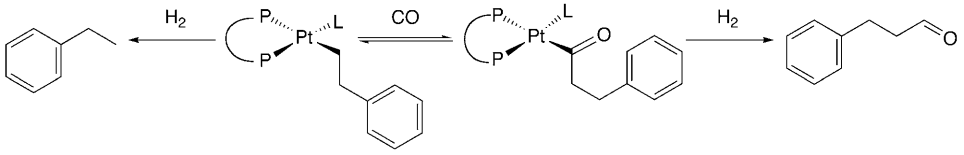

We further observed that the branched-to-linear ratio decreases with increasing reaction temperature. At lower temperatures, the secondary α-methylbenzyl intermediate **8** is more stable than the phenethyl intermediate **9** by 4–6 kJ/mol, as has been shown for similar systems by *Rappé* and co-workers (*Fig. 4*) [42]. The α-methylbenzyl intermediate **8** will, therefore, be the preferred intermediate at lower temperature. However, at higher temperature, the sterically less demanding phenethyl intermediate **9** is expected to be the predominant species due to the bigger conformational

space of the ligand framework resulting in an increased steric interaction with the substrate [43]. Moreover, secondary-alkyl-coordinated Pt-complexes are more prone to β-H elimination than primary-alkyl-coordinated ones, thus leading to the reformation of the substrate at higher temperatures and removal of the branched-alkyl Pt-species and slow formation of the branched aldehyde [1][41]. Whether the η^3-complex **10** plays a role as an intermediate is still a matter of debate, since π-acceptor ligands like phosphonites usually favor the formation of η^3-complexes, rather than η^1-alkyl species.

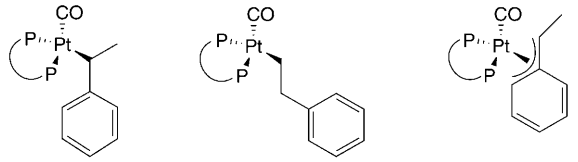

8 **9** **10**

Fig. 4. *Intermediates* **8**–**10** *of the Hydroformylation Reaction*

Furthermore, the enantioselectivity in the hydroformylation of styrene (**4a**) is found to be temperature-dependent, eventually leading to enantiomer inversion with increasing reaction temperature (see *Table 4*). An inversion of the enantioselectivity is observed for all applied pressures, but the inversion temperature is pressure-dependent. The inversion of enantioselectivity has been observed before by *Kollar et al.* [44] in the Pt/Sn-catalyzed asymmetric hydroformylation of styrene and has recently been studied in more detail by *Casey et al.* [41]. Since the energy difference between the enantiomeric pathways remains in the same order of magnitude with increasing pressure, the effects of temperature and pressure are difficult to distinguish on this scale. However, the observed conformation of the complex [$PtCl_2$(**1**)] is prone to changes under influence of solvent, temperature, and pressure, and the information obtained from the solid-state structure cannot directly be related with the stereoselection process.

We were further interested in the hydroformylation of the substrates 4-methylstyrene (**4b**), allyl acetate (**4d**), and vinyl acetate (**4c**) (*Scheme 1*). With **4b**, less hydrogenation was observed compared to styrene (**4a**) as a substrate, but no clear trend was observed in the stereoselection process under comparable reaction conditions, although higher branched-to-linear ratios could be observed with 4-methylstyrene under the same conditions (*Table 5*).

Interestingly, the hydroformylation of allyl acetate (**4d**) and vinyl acetate (**4c**) gave much better results in terms of enantioselectivity compared to the styrene derivatives. Thus, 80% ee was achieved in the hydroformylation of **4d** at 20 bar CO/H_2 and 40°. Also when applying different reaction conditions, still high ee for the branched product were observed. A clear drawback, however, is the fact that the chemoselectivities (hydrogenation *vs.* hydroformylation) as well as the regioselectivities towards the desired branched aldehyde are quite low and have to be improved considerably (*Table 6*). Moreover, unwanted side reactions leading to unidentified products occurred

Table 5. *Enantioselective Hydroformylation of 4-Methylstyrene* (**4b**) *with (*R*)-***3***[a])*

p [bar]	*T* [°]	*t* [h]	Conversion [%]	Hydrogenation [%][b])	b/l[c])	ee [%]
10	80	2	61	46	43:57	12.4
20	80	2	100	40	61:39	3.1
60	80	2	100	33	71:29	4.7
60	40	2	85	21	78:22	4.8

[a]) Reaction conditions: ligand/Pt/$SnCl_2$ 1:1:1, substrate/Pt 1000:1, CO/H_2 1:1, CH_2Cl_2; preformation: 2 h at 20 bar, 60°. [b]) Formation of **7b**. [c]) Ratio **5b**/**6b**, *i.e.*, branched/linear aldehyde.

Table 6. *Enantioselective Hydroformylation of Allyl Acetate* (**4d**) *and Vinyl Acetate* (**4c**) *with (*R*)-***3***[a])*

	p [bar]	*T* [°]	*t* [h]	Conversion [%]	Hydroformylation [%]	Hydrogenation [%][b])	b/l[c])	ee [%]
4d	10	80	12	61	20	13	9:91	75
	20	40	64	100	47	25	13:87	80
	20	80	12	100	34	24	11:89	79
	40	80	12	100	35	31	13:87	74
	60	80	12	100	33	30	12:88	71
	10	80	64	36	5	31	22:78	58 (*R*)
4c	20	80	64	82	14	18	28:72	67 (*R*)
	40	80	64	99	21	22	28:72	75 (*R*)
	60	80	64	100	21	28	21:79	77 (*R*)

[a]) Reaction conditions: ligand/Pt/$SnCl_2$ 1:1:1, substrate/Pt 1000:1, CO/H_2 1:1, CH_2Cl_2; preformation: 2 h at 20 bar, 60°. [b]) Formation of **7d** or **7c**, resp. [c]) Ratio **5d**/**6d** or **5c**/**6c**, resp., *i.e.*, branched/linear aldehyde.

in some cases, accounting for the observed discrepancies in conversion and product distribution.

Also in the hydroformylation of vinyl acetate (**4c**), and under different reaction conditions, moderate to good enantioselectivities of up to 77% were obtained. Also in this case, low selectivities towards the desired branched aldehyde were observed (*Table 6*) (for an inversion of the linear-to-branched ratio in the asymmetric hydroformylation, see [45]).

Conclusions. – The complexes [$PtCl_2${(*R*,*R*)-XantBino}] ((*R*)-**2**) and [$PtCl_2${(*S*,*S*)-XantBino}] ((*S*)-**2**) were prepared, and the latter one was characterized by means of X-ray crystal-structure analysis, revealing an unusual 'out-of-plane' Pt-core in the solid-state structure, which was further supported by NMR data. Reaction of (*R*)-**2** with 1 equiv. of $SnCl_2$ afforded the corresponding Pt/Sn complex [$PtCl(SnCl_3)${(*R*,*R*)-XantBino}] ((*R*)-**3**), which was characterized by ^{31}P-NMR spectroscopy. This complex was used as precatalyst for the asymmetric hydroformylation of styrene (**4a**), 4-methylstyrene (**4b**), vinyl acetate (**4c**), and allyl acetate (**4d**). In the case of **4a** as substrate, chemoselectivities of up to 75%, regioselectivities of up to 83%, and enantioselectivities of up to 30% were reached, while high ee of 80 and 77% were reached for the substrates allyl acetate (**4d**) and vinyl acetate (**4c**), respectively. The enantioselectivity was found to be independent of the conversion, meaning that no racemization occurs as a conse-

quence of the stoichiometric amount of $SnCl_2$ with respect to the Pt-complex **2**. On the basis of the reaction mechanism, the temperature and pressure dependency of the hydroformylation is explained. For styrene (**4a**) as a substrate, concerning enantioselectivity, an inversion of the stereoselection process was found with increasing temperature, which is attributed to conformational changes in the catalyst structure at elevated temperature.

Umicor is kindly acknowledged for a generous loan of precious metals for our studies.

Experimental Part

General. All reactions were performed under Ar by using standard *Schlenk* techniques. Chemicals were purchased from *Aldrich Chemical Co.*, *Acros* or *VWR*. Solvents were purified by passing them through basic alumina columns after degassing. Styrene was purified by passage through basic alumina and distilled prior to use. $PtCl_2$ was obtained from *OMG*. Synthesis gas *5.0* (CO/H_2 50 : 50) was purchased from *HoekLoos*. GC: *Shimadzu GC-17A*, *HP-Ultra-2* column (25 m × 0.25 mm), FID detector; determination of the enantiomeric excess (ee) with *Carlo Erba GC6000 Vega 2*, *Lipodex-E* column (25 m × 0.25 mm), FID detector. NMR Spectra: *Varian-Mercury-400* spectrometer; δ in ppm, J in Hz.

*Crystal-Structure Determination of [PtCl$_2${(S)-**1**}]* ((*S*)-**2**). The crystal data were collected (out to $\sin(\theta/\lambda) = 0.65$ Å^{-1}) on a *Nonius-KappaCCD* diffractometer with rotating anode by using graphite-monochromated MoK_α radiation. A face-indexed absorption correction was applied with PLATON/ABSTOMPA (transmission range 0.508–0.844) [46]. The structure was solved by direct methods with SHELXS97, and was refined on F^2 by least-squares procedures with SHELXL97 [46]. All non-H-atoms were refined with anisotropic displacement parameters. H-Atoms were constrained to idealized geometries and allowed to ride on their carrier atoms with isotropic displacement parameter related to the equivalent replacement parameter of their carrier atoms. The crystal structure contains solvent-accessible voids with a total volume of 1339 Å^3 per unit cell volume filled with disordered solvent molecules (CH_2Cl_2/MeCN). Their contribution to the structure factors was ascertained by using PLATON/SQUEEZE [47]. Structure validation and molecular-graphics preparation were performed with the PLATON package [47]. Selected bond lengths, distances, and bond angles are given in *Table 1*. Crystal data (excluding disordered solvent): $C_{55}H_{36}Cl_2O_5P_2Pt$, M 1104.76, orthorhombic, $a = 11.2545(1)$, $b = 17.1813(1)$, $c = 17.4069(2)$ Å, $V = 5299.59(7)$ Å^3, T 150 K, space group $P2_12_12_1$ (no. 19), $Z = 4$, μ(MoK_α) = 2.853 mm^{-1}, 60343 reflections collected, 12174 unique ($R_{int} = 0.062$) which were used in all calculations. $R_1 = 0.0302$, $wR_2 = 0.0749$, $s = 1.05$, *Flack* = 0.012(4), ρ(min) = −0.67, ρ(max) = 0.75 e/Å^3.

CCDC-295949 contains the supplementary crystallographic data for this paper. These data can be obtained free of charge *via* http://www.ccdc.cam.ac.uk/data_request/cif from the *Cambridge Crystallographic Data Centre*.

*(11b*R*,11′b*R*)-4,4′-(9,9-Dimethyl-9*H*-xanthene-4,5-diyl)bis[dinaphtho[2,1-*d*:1′,2′-*f*][1,3,2]dioxaphosphepin]* ((*R,R*)-XantBino); (*R*)-**1**). The synthesis of this ligand and the analogous (*S,S*)-isomer (*S*)-**1** was carried out as previously described [18b][20]. ^{1}H-NMR ($CDCl_3$): 7.94 (*d*, $J = 8.8$, 2 bino H); 7.90 (*d*, $J = 8.0$, 2 bino H); 7.84 (*d*, $J = 8.0$, 2 bino H); 7.63 (*d*, $J = 8.8$, 2 bino H); 7.58 (*d*, $J = 8.8$, 2 bino H); 7.55 (*dd*, $J = 8.0$, $J = 0.8$, 2 bino H); 7.42 (*t*, $J = 8.8$, 6 xant H); 7.32 (*d*, $J = 8.4$, 2 bino H); 7.28 (*d quint.*, $J = 8.0$, 1.2, 4 bino H); 7.18 (*d*, $J = 8.8$, 2 bino H); 6.92 (*s*, $J = 8.8$, 2 bino H); 6.90 (*d*, $J = 7.2$, 4 bino H); 1.79 (*s*, Me_2C). ^{13}C{^{1}H}-NMR ($CDCl_3$): 152.6; 149.9; 149.1; 133.0; 132.5; 131.5; 130.9; 130.4; 129.9; 129.0 (*d*, J(P,C) = 16.8); 128.5; 128.2 (d, J(P,C) = 6.8); 126.9 (*d*, J(P,C) = 3.8); 125.8 (*d*, J(P,C) = 19.0); 124.6 (*d*, J(P,C) = 20.6); 123.3; 121.9 (*d*, J(P,C) = 5.3); 34.1 (Me_2C); 31.9 (Me_2C). ^{31}P{^{1}H}-NMR ($CDCl_3$): 178.0 (*s*).

*(*SP*-4-2)-Dichloro{(11b*R*,11′b*R*)-4,4′-(9,9-dimethyl-9*H*-xanthene-4,5-diyl)bis[dinaphtho[2,1-*d*:1′2′-*f*]-[1,3,2]dioxaphosphepin-*κ*P^4]}platinum* ([$PtCl_2${(*R*)-**1**}]; (*R*)-**2**). [$PtCl_2(MeCN)_2$] was prepared by refluxing $PtCl_2$ in MeCN for 2 h. Subsequently, 1 equiv. of the ligand (*R*)-**1** was added and the reaction continued for 1 h under reflux, during which a white precipitate formed. Filtration at r.t. gave (*R*)-**2**. White powder.

Alternatively, [$PtCl_2$(cod)] (72.3 mg, 193.2 μmol) and, *e.g.*, (*S*)-**1** (172.3 mg, 205.3 μmol) were dissolved in CH_2Cl_2 (15 ml) and stirred for 1 h at r.t., yielding (*S*)-**2** as a white precipitate. Colorless, block-shaped crystals were obtained after slow diffusion of MeCN (15 ml) into a CH_2Cl_2/$CHCl_3$ soln. (5 ml/4 ml). Yield 82%. $^{31}P\{^1H\}$-NMR ($CDCl_3$): 110.5 (*d*, *J*(P,P) = 15.9, *J*(Pt,P) = 5000); 113.1 (*d*, *J*(P,P) = 15.9, *J*(Pt,P) = 5040). Anal. calc. for $C_{55}H_{36}Cl_2O_5P_2Pt$: C 59.79, H 3.28; found: C 59.84, H 3.42.

*(*SP*-4-3)-Chloro{(11b*R*,11′b*R*)-4,4′-(9,9-dimethyl-9*H*-xanthene-4,5-diyl)bis[dinaphtho[2,1-*d*:1′,2′-*f*][1,3,2]dioxaphosphepin-κP^4]}(trichlorostannyl)platinum* ((*R*)-**3**). To $SnCl_2$ (2.6 mg, 13.7 μmol), an equimolar amount of Pt-complex (*R*)-**2** (15 mg, 13.7 μmol), dissolved in CH_2Cl_2 (10 ml), was added. After 2 h, a yellow soln. was obtained. Of this solution, 10 ml was taken, and the solvent was evaporated. The residue was redissolved in $CDCl_3$ (0.5 ml), and a ^{31}P-NMR was recorded at −50°. $^{31}P\{^1H\}$-NMR ($CDCl_3$): 124.7 (*d*, *J*(P,P) = 15.2, *J*(Pt,P) = 4904, *J*(Sn,P) = 197); 132.8 (*d*, *J*(P,P) = 15.2, *J*(Pt,P) = 4108, *J*(Sn,P) = 5856, 5596).

Hydroformylation of Styrene (**4a**). The soln. (10 ml) of (*R*)-**3** in CH_2Cl_2 (see above) was transferred to a 75-ml stainless steel autoclave equipped with a stirring bar. Additional CH_2Cl_2 (10 ml) was added. The autoclave was pressurized to 20 bar and heated to 60°. After 2 h of preformation, **4a**/decane (1.6 g/0.5 g, 15.4 mmol/3.4 mmol), dissolved in CH_2Cl_2 (5 ml), was added at the desired pressure and temp. The pressure was kept constant by using a gas line with a pressure regulator. After the reaction, the autoclave was cooled to r.t., depressurized, and the mixture was analyzed by GC to determine the conversion and the chemo- and regioselectivities.

To a soln. of $LiAlH_4$ (0.12 g) in Et_2O (15 ml), the above mixture (5 ml) was added. After 3 h, the reaction was quenched with H_2O, the mixture extracted with Et_2O (3 × 30 ml), the combined org. layer dried ($MgSO_4$) and evaporated, and the residue dissolved in CH_2Cl_2 (5 ml) and treated with trifluoroacetic anhydride (1,5 ml). The solvent and excess trifluoroacetic anhydride were evaporated, and the residue was dissolved in toluene and analyzed by GC.

Hydroformylation of 4-Methylstyrene (**4b**)*, Vinyl Acetate* (**4c**)*, and Allyl Acetate* (**4d**). Catalysis experiments were performed simultaneously in the parallel autoclave system *AMTEC SPR16* [48], equipped with pressure sensors and a mass-flow controller and suitable for monitoring and recording gas uptakes throughout the reactions. General procedure for the catalysis experiments: Four stainless-steel autoclaves of the *AMTEC SPR16* were heated to 90° and flushed with Ar (15 bar) four times. Subsequently, the reactors were cooled to r.t. and flushing with Ar was repeated again for four times. The reactors were charged each with the soln. of the precatalyst (see below) dissolved in CH_2Cl_2 under Ar. The atmosphere was further exchanged with synthesis gas (CO/H_2 1:1) (gas exchange cycle 1), and the reactors were pressurized with CO/H_2 to 10 bar. After heating to 60°, the pressure was increased to 20 bar and kept constant during the preformation time. Subsequently, the substrate was injected *via* syringe, and the final pressure and temperature were adjusted. In case of **4a**, **4b**, and **4d**, decane was used as an internal standard. In the case of **4c**, ethyl propanoate was used as the internal standard. At the end of the catalysis experiments, the reactors were cooled to r.t., and the autoclave contents were analyzed by means of GC.

REFERENCES

[1] S. Castillón, E. Fernández, in 'Rhodium Catalyzed Hydroformylation', Eds. P. W. N. M. van Leeuwen and C. Claver, Kluwer, Amsterdam, 2000, p. 145.
[2] C. D. Frohning, C. W. Kohlpainter, in 'Applied Homogeneous Catalysis with Organometallic Compounds: A Comprehensive Handbook', Eds. B. Cornils and W. A. Herrmann, Wiley-VCH, Weinheim, 1996, p. 27.
[3] C. Botteghi, G. Consiglio, P. Pino, *Chimia* **1972**, *26*, 141.
[4] C. Y. Hsu, M. Orchin, *J. Am. Chem. Soc.* **1975**, *97*, 3553.
[5] M. Tanaka, Y. Watanabe, T. A. Mitsudo, K. Yamamoto, Y. Takegami, *Chem. Lett.* **1972**, 483.
[6] P. Haelg, G. Consiglio, P. Pino, *Helv. Chim. Acta* **1981**, *64*, 1865.
[7] C. U. Pittmann, Y. Kawabata, L. I. Flowers, *J. Chem. Soc., Chem. Commun.* **1982**, 473.
[8] G. Parinello, J. K. Stille, *J. Am. Chem. Soc.* **1987**, *109*, 7122.
[9] J. K. Stille, H. Su, P. Brechot, G. Parrinello, L. S. Hegedus, *Organometallics* **1991**, *10*, 1183.

[10] C. D. Fernández, M. I. García-Seijo, T. Kégl, G. Petöcz, L. Kollár, M. E. García-Fernández, *Inorg. Chem.* **2002**, *41*, 4435.
[11] F. Agbossou, A. Mortreux, *Chem. Rev.* **1995**, *95*, 2484.
[12] C. Claver, P. W. N. M. van Leeuwen, in 'Rhodium Catalyzed Hydroformylation', Eds. P. W. N. M. van Leeuwen and C. Claver, Kluwer, Amsterdam, 2000, p. 107.
[13] N. Sakai, S. Mano, K. Nozaki, H. Takaya, *J. Am. Chem. Soc.* **1993**, *115*, 7033.
[14] J. E. Babin, G. T. Whiteker, to *Union Carbide Corp.*, Pat. WO 93/03830, 1992.
[15] G. J. H. Buisman, M. E. Martin, E. J. Vos, A. Klootwijk, P. C. J. Kamer, P. W. N. M. van Leeuwen, *Tetrahedron: Asymmetry* **1995**, *6*, 719.
[16] P. Meessen, D. Vogt, W. Keim, *J. Organomet. Chem.* **1998**, *551*, 165.
[17] W. Goertz, P. C. J. Kamer, P. W. N. M. van Leeuwen, D. Vogt, *Chem.–Eur. J.* **2001**, *7*, 1614.
[18] a) J. I. van der Vlugt, R. Sablong, P. C. M. M. Magusin, A. M. Mills, A. L. Spek, D. Vogt, *Organometallics* **2004**, *23*, 3177; b) J. I. van der Vlugt, J. M. J. Paulusse, E. J. Zijp, J. A. Tijmensen, A. M. Mills, A. L. Spek, C. Claver, D. Vogt, *Eur. J. Inorg. Chem.* **2004**, 4193.
[19] W. Goertz, Ph.D. Thesis, RWTH Aachen, 1998.
[20] J. I. van der Vlugt, A. C. Hewat, S. Neto, R. Sablong, A. M. Mills, A. L. Spek, C. Müller, D. Vogt, *Adv. Synth. Catal.* **2004**, *346*, 993.
[21] M. T. Reetz, M. Pastó, *Tetrahedron Lett.* **2000**, *41*, 3315; M. T. Reetz, A. Gosberg, D. Moulin, *Tetrahedron Lett.* **2002**, *43*, 1189.
[22] C. Claver, E. Fernandez, A. Gillon, K. Heslop, D. J. Hyett, A. Martorell, A. G. Orpen, P. G. Pringle, *Chem. Commun.* **2000**, 961.
[23] D. Selent, K.-D. Wiese, D. Röttger, A. Börger, *Angew. Chem., Int. Ed.* **2000**, *39*, 1639; C. Kunze, D. Selent, I. Neda, M. Freytag, P. G. Jones, R. Schmutzler, W. Baumann, A. Börner, *Z. Anorg. Allg. Chem.* **2002**, *628*, 779.
[24] O. Lot, I. Suisse, A. Mortreux, F. Agbossou, *J. Mol. Catal. A: Chem.* **2000**, *164*, 125; S. Naili, I. Suisse, A. Mortreux, F. Agbossou-Niedercorn, G. Nowogrocki, *J. Organomet. Chem.* **2001**, *628*, 114.
[25] J. I. van der Vlugt, R. Sablong, A. M. Mills, H. Kooijman, A. L. Spek, D. Vogt, *Dalton Trans.* **2003**, 4690.
[26] D. Haag, J. Runsink, H. D. Scharf, *Organometallics* **1998**, *17*, 398.
[27] M. T. Reetz, X. Li, *J. Am. Chem. Soc.* **2006**, *128*, 1044.
[28] L. Dahlenburg, S. Mertel, *J. Organomet. Chem.* **2001**, *630*, 221.
[29] D. Selent, W. Baumann, R. Kempe, A. Spannenberg, D. Röttger, K. D. Wiese, A. Börner, *Organometallics* **2003**, *22*, 4265.
[30] W. Ahlers, D. Wiebelhaus, R. Paciello, M. Bartsch, R. Baumann, D. Vogt, A. C. Hewat, to *BASF AG*, Pat. WO 0222261-A2, 2002.
[31] J. Bakos, S. Cserépi-Szücs, Á. Gömöry, C. Hegedüs, L. Markó, Á. Szöllösy, *Can. J. Chem.* **2001**, *79*, 725; S. Cserépi-Szücs, J. Bakos, *Chem. Commun.* **1997**, 635.
[32] C. J. Cobley, P. G. Pringle, *Inorg. Chim. Acta* **1997**, *265*, 107.
[33] L. A. van der Veen, P. K. Keeven, P. C. J. Kamer, P. W. N. M. van Leeuwen, *Dalton Trans.* **2000**, *13*, 2105.
[34] D. J. Adams, D. J. Cole-Hamilton, D. A. J. Harding, E. G. Hope, P. Pogorzelec, A. M. Stuart, *Tetrahedron* **2004**, *60*, 4079.
[35] G. Petöcz, Z. Berente, T. Kégl, L. Kollár, *J. Organomet. Chem.* **2004**, *689*, 1188.
[36] G. Franciò, C. G. Arena, F. Faraone, C. Graiff, M. Lanfranchi, A. Tiripicchio, *Eur. J. Inorg. Chem.* **1999**, 1219.
[37] a) L. A. van der Veen, P. K. Keeven, G. C. Schoemaker, J. N. H. Reek, P. C. J. Kamer, P. W. N. M. van Leeuwen, M. Lutz, *Organometallics* **2000**, *19*, 872; b) J. I. van der Vlugt, M. M. P. Grutters, A. M. Mills, H. Kooijman, A. L. Spek, D. Vogt, *Eur. J. Inorg. Chem.* **2003**, 4361; c) J. I. van der Vlugt, J. Ackerstaff, T. W. Dijkstra, A. M. Mills, H. Kooijman, A. L. Spek, A. Meetsma, H. C. L. Abbenhuis, D. Vogt, *Adv. Synth. Catal.* **2004**, *346*, 399.
[38] P. Haelg, G. Consiglio, P. Pino, *J. Organomet. Chem.* **1985**, *296*, 281.
[39] A. Scrivanti, C. Botteghi, L. Toniolo, A. Berton, *J. Organomet. Chem.* **1988**, *344*, 261; P. S. Pregosin, S. N. Sze, *Helv. Chim. Acta* **1978**, *61*, 1848.

[40] V. S. Petrosyan, A. B. Permin, V. I. Bogdashkina, D. P. Krut'ko, *J. Organomet. Chem.* **1985**, *292*, 303.
[41] C. P. Casey, S. C. Martins, M. A. Fagan, *J. Am. Chem. Soc* **2004**, *126*, 5585.
[42] L. A. Castonguay, A. K. Rappé, C. J. Casewit, *J. Am. Chem. Soc.* **1991**, *113*, 7177.
[43] K. Angermund, W. Baumann, E. Dinjus, R. Fornika, H. Goerls, M. Kessler, C. Krueger, W. Leitner, F. Lutz, *Chem.–Eur. J.* **1997**, *3*, 755.
[44] L. Kollár, J. Bakos, I. Tóth, B. Heil, *J. Organomet. Chem.* **1988**, *350*, 277.
[45] V. F. Slagt, Ph.D. Thesis, University of Amsterdam, 2003.
[46] G. M. Sheldrick, 'SHELXS97, SHELXL97', University of Göttingen, Göttingen, 1997.
[47] A. L. Spek, *J. Appl. Crystallogr.* **2003**, *36*, 7.
[48] www.amtec-chemnitz.de.

Received January 31, 2006